doi:10.1038/nature10612

1. Supplementary Notes

1.1 Data and data analysis

The analysis of the three stars presented in this report is based on 510 days of consecutive photometric observations (quarters Q0-Q6) with the *Kepler* satellite[24] in the long cadence mode (about 30 min)[22] with a duty cycle of about 92%. None of the stars fell on the *Kepler*-CCD 3 module after it was broken. Infrequent gaps in the time series occurred when the spacecraft was in safe mode. Periodic gaps originate from *Kepler* pointing towards Earth for data downlink every 30 days. This leads to a spectral window very close to the ideal case (Supplementary Fig. 11). This window function cannot produce alias peaks that could be confused with components of rotational multiplets. The photometric band-pass of *Kepler* is roughly equivalent with a broad-band white light filter. The Fourier spectra have been computed from the photometric time series corrected for instrumental artifacts[22].

The initial sample that was searched for rotational splitting consisted of about 100 stars. Larger radii lead to smaller frequency separations, that are harder to measure in the power spectrum. We thus limited our investigation to a sample of giants with relatively small radii, i.e., to those stars which have their power excess located at frequencies higher than 90 μHz. The sampling rate of the long-cadence mode restricts the sensitivity to frequencies below ~280 μHz (Nyquist frequency). This frequency domain corresponds to low-luminosity red-giant stars[21].

The linewidth of the mode profiles has been determined by fitting individual Lorentzian profiles to the component of a rotationally split mode with the highest signal-to-noise ratio (Fig. 3 and Supplementary Figs. 9 and 10). The modes in the outer wings of the dipole forest have very

narrow mode peaks (Supplementary Fig. 1). The width of the most narrow modes with dominant g-mode character are limited by the frequency resolution (~0.02 μHz). This value implies an upper limit for the mode width and thus a lower limit for the mode lifetime.

Stellar rotation lifts the degeneracy of non-radial modes, producing a multiplet of (2ℓ+1) frequency peaks in the power spectrum for each mode, where ℓ is the spherical degree of a given mode. In the case of slow rigid rotation the components of a rotationally split multiplet are separated in frequency by an amount $\delta f = m \cdot \Omega \cdot \beta_{nl} = m \cdot \Omega \cdot (1\text{-}C_{nl})$, where Ω is the rotational frequency, m is the azimuthal order of the mode, and C_{nl} is the so-called Ledoux constant[23] whose value varies for different degrees of mixing between acoustic and gravity modes. The amplitude ratios of modes with different values of |m| are governed from the inclination of the rotation axis towards the observer[25]. The application of this principle is explored in more detail in the next section.

We obtained several spectra of KIC 8366239 and KIC 5356201 with the HERMES spectrograph, mounted to the 1.2 m Mercator telescope at La Palma, Canary Islands, Spain[26]. By co-adding individual spectra of each star, we reached a signal-to-noise level of about 40 in the averaged spectrum, which is sufficient to derive the line broadening rotational velocity[27] (Tab. 1).

1.2 Details on modelling KIC 8366239

The models were computed with the code ATON (Ref: 28). The representative model of KIC 8366239 was taken from the grid of models and frequencies previously computed[12]. We choose a model with values of the frequency excess ν_{max} and large frequency separation $\Delta\nu$ close to the

values derived from the power spectrum of KIC 8366239. Therefore, the model is compatible in stellar mass and radius to KIC 8366239.

The global properties of the model are: M=1.4 $M_{\odot}$, R=5.1 $R_{\odot}$, chemical composition Z=0.02, Y=0.278, and the standard solar mixture[29]. The model was computed using the mixing length (MLT) treatment of convection with the mixing length parameter α_{mlt}=1.9. The model has an age of $3.6 \cdot 10^{9}$ yr, a luminosity ~ 12.24 $L_{\odot}$ and is in the H-shell burning phase. The mass of its inert He core is 0.19 $M_{\odot}$. The computation was done with a very small diffusive overshooting[30] ($\zeta=1 \cdot 10^{-4}$) from the convective core during the main sequence.

1.3 Three firm cases of rotational splitting

Besides KIC 8366239 (Fig. 1), we also show two additional stars with firm detections of rotational splitting (Tab. 1), KIC 5356201 and KIC 12008916. From the location of the frequency excess ν_{max} (Supplementary Table 1) and the period spacing of the dipole mixed modes (Tab. 1), we conclude that all three stars are in the hydrogen-shell burning phase. Also in KIC 5356201 (Supplementary Figs. 3 and 4) we find that the modes at the centre of the dipole forest have broader linewidths, hence shorter lifetimes and exhibit smaller rotational splitting than the modes with long lifetimes (narrow mode profiles) in the wings of the forest (Supplementary Figs. 9 and 10). KIC 12008916 (Supplementary Figs. 5 and 6) has in general very narrow mode profiles. Among the three stars, we also find the largest splitting in this star.

Pure acoustic modes exhibit a constant frequency spacing, which can be described by the large frequency separation $\Delta\nu$ between modes of the same spherical degree ℓ. To investigate the

structure of this so-called comb-like pattern, we folded the power spectrum with the large frequency separation. In the resulting échelle diagrams pressure modes of the same spherical degree form nearly vertical ridges. This is the case for the radial and hence pure acoustic mode (ℓ=0, green squares) and the quadrupole mode (ℓ=2, red triangles) for which the mixing is less prominent. For dipole modes (ℓ=1, blue dots) we find a dense mode forest instead of a single vertical ridge as a result of the mixed modes. The échelle diagram of KIC 8366239 (Supplementary Fig. 2) clearly shows doublets for the rotationally split modes. However, the centre of the doublets follows the same pattern as shown for mixed modes in KIC 6928997 (Ref: 3). Similar échelle diagrams are shown for KIC 5356201 (Supplementary Fig. 4) and KIC 12008916 (Supplementary Fig. 6).

Comparing the three stars, we find different multiplet geometries. The amplitude ratio of a rotationally split mode depends on the inclination of the rotation axis towards the observer. This was considered for solar-like stars[25] and leads to varying amplitude ratios among modes of different azimuthal order |m| of a split multiplet. In principle this property can be used to derive the inclination of the stellar rotation axis, whereby dipole modes should follow the general scheme, presented in Supplementary Table 2.

As the multiplets found in the three stars appear not to have equal heights, we are limited to a rather rough estimate of the inclination determination which is sufficient to describe the three cases presented in this work. This has no influence on our interpretation. For KIC 8366239 and KIC 12008916 we find a doublet structure in the split dipole modes. In some cases we find a weak signature of the m=0 peak indicating an inclination around 70° for both stars. A different

geometry is found in KIC 5356201, where the dipole modes clearly show triplets with roughly equal amplitudes, indicating an inclination angle between 20° and 70°. We note that the determination of the equatorial surface rotation velocity is unaffected by any assumptions about the inclination, as the rotational frequency separation of modes with consecutive azimuthal order ($|\Delta m|=1$) is independent of the orientation of the star towards the observer.

Although the modes of the same azimuthal order $|m|$ are expected to have similar amplitudes[25], we find differences in the heights of the multiplet peaks of the split dipole modes, e.g. in the frequency spectrum of KIC 8366239 between 185 and 198 μHz (Supplementary Fig.1). In KIC 5356201, these asymmetry effects lead to missing peaks of the triplet in the wings of the dipole forest (Supplementary Figs. 3a, 4 and 9). To avoid contamination of our results through these incomplete multiplets, we show them as open symbols in Supplementary Figs. 4 and 9 but excluded them from the further analysis, as their splitting is insecure by a factor of 2. From studying time resolved oscillation spectra as well as subsets, we argue that this issue of completeness and asymmetry is related to the long lifetimes of the stochastically exited mixed modes. As not all individual mode peaks of a rotationally split multiplet are exhibiting detectable mode heights at all times. This leads to the asymmetry in the final oscillation spectrum.

2. Supplementary References

24. Koch, D.G., *et al. Kepler* Mission Design, Realized Photometric Performance, and Early Science. *Astrophys.J* **713**, L79 (2010).

25. Gizon, L. & Solanki, S.K. Determining the inclination of the rotation axis of a sun-like star. *Astrophysical Journal* **589**, 1009 (2003).

26. Raskin, G., *et al*, HERMES: a high-resolution fibre-fed spectrograph for the Mercator telescope. *Astronomy & Astrophysics* **526**, A69. (2011).

27. Hekker, S. & Melendez, S. Precise radial velocities of giant stars. *Astronomy & Astrophysics* **475**, 1003 (2007).

28. Ventura, P., D'Antona, F., Mazzitelli, I. The ATON 3.1 stellar evolutionary code. A version for asteroseismology. *Astrophysics and Space Science*, **316**, 93-98 (2008)

29. Grevesse, N. & Noels, A., La composition chimique du Soleil. in Hauck B., Paltani S.R.D., eds., La Formation des Elements Chimiques. AVCP, 205-257 (1993)

30. Ventura, P., Zeppieri, A., Mazzitelli, I., D'Antona, F., Full spectrum of turbulence convective mixing: I. theoretical main sequences and turn-off for 0.6 \ 15 Msolar. Astronomy and Astrophysics, v.334, p.953-968 (1998)

3. Supplementary Tables

KIC	ν_{max} [μHz]	$\Delta\nu$ [μHz]	Radius [$R_\odot$]	Mass [$M_\odot$]	T_{eff} Aster. [K]	T_{eff} Spec. [K]	Inclination range
8366239	182 ± 1	13.66 ± 0.02	5.30 ± 0.08	1.49 ± 0.07	4980 ± 120	4910±80	High
5356201	209.7 ± 0.7	15.83 ± 0.02	4.47 ± 0.03	1.23 ± 0.04	4840 ± 90	4750±60	Intermed.
12008916	159.9 ± 0.6	12.85 ± 0.01	5.18 ± 0.05	1.26 ± 0.03	4830 ± 100	-	High

Supplementary Table 1. Stellar parameters computed from asteroseimological scaling laws. The frequency of maximum oscillation power and the average large frequency separation are given by ν_{max} and $\Delta\nu$. The radius, mass and effective temperature were computed from scaling laws[17]. For the two stars for which we have obtained ground-based spectroscopy, we also provide the effective temperature, derived from the spectra. The last column gives the estimate of the inclination as defined in Supplementary Table 2.

Inclination range	**Shape of dipole (ℓ=1) modes**	
[degree]	Visible peaks	Appearance
Large: ~70-90	m=±1	Doublet
Intermediate: ~20-70	m=±1, m=0	Triplet
Small: ~0-20	m=0	Single peak

Supplementary Table 2. Dependencey of mode geometry on the inclination of the rotation axis. Schematic description of the expected geometry of a rotationally split dipole mode in the power spectrum following[25]. Only mode peaks which reach substantial heights are given.

4. Supplementary Figures and Legends

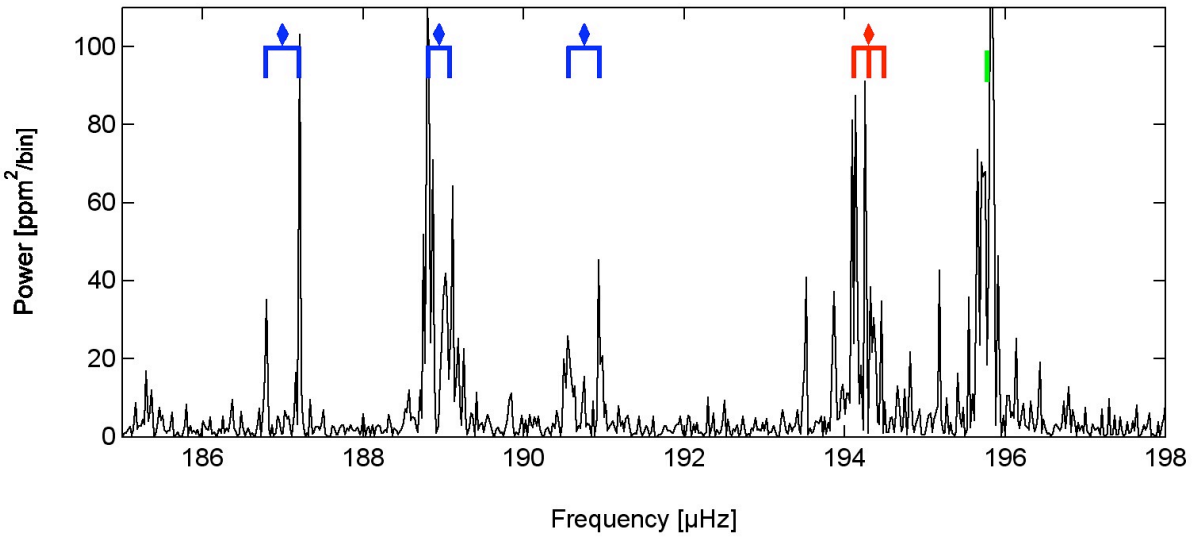

Supplementary Figure 1. Frequency spectrum centred on the radial order with the best signal-to-noise ratio of KIC 8366239. Individual mode peaks of degree ℓ=0, ℓ=1 and ℓ=2 are marked by green, blue and red vertical ticks, respectively. Modes, which belong to one multiplet are connected with a horizontal bar. The central frequency of each split multiplet is indicated through a diamond on top. For the analysis, only clearly identified dipole mode doublets have been used. While the central split dipole mode has the broadest Lorentzian profiles (hence shorter lifetime) the two outer split modes have narrower peaks and therefore longer lifetimes.

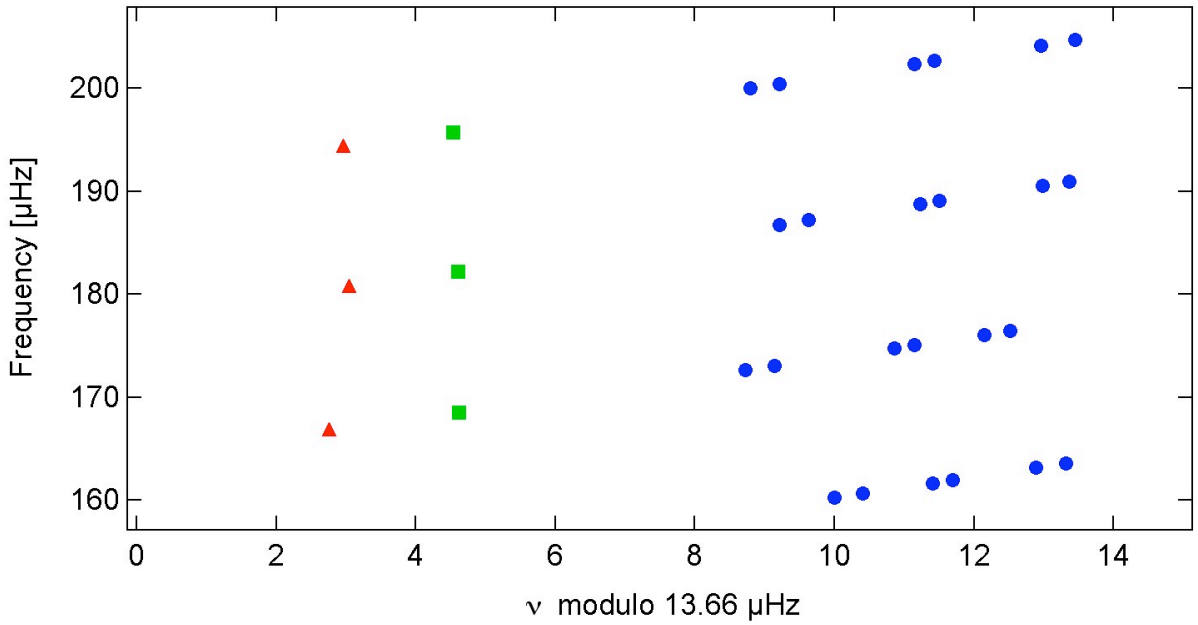

Supplementary Figure 2. The échelle diagram of KIC 8366239. Modes of degree ℓ=0, ℓ=1 and ℓ=2 are marked with green squares, blue dots and red triangles, respectively. The construction and interpretation of an échelle diagram are described in the Supplementary Discussions

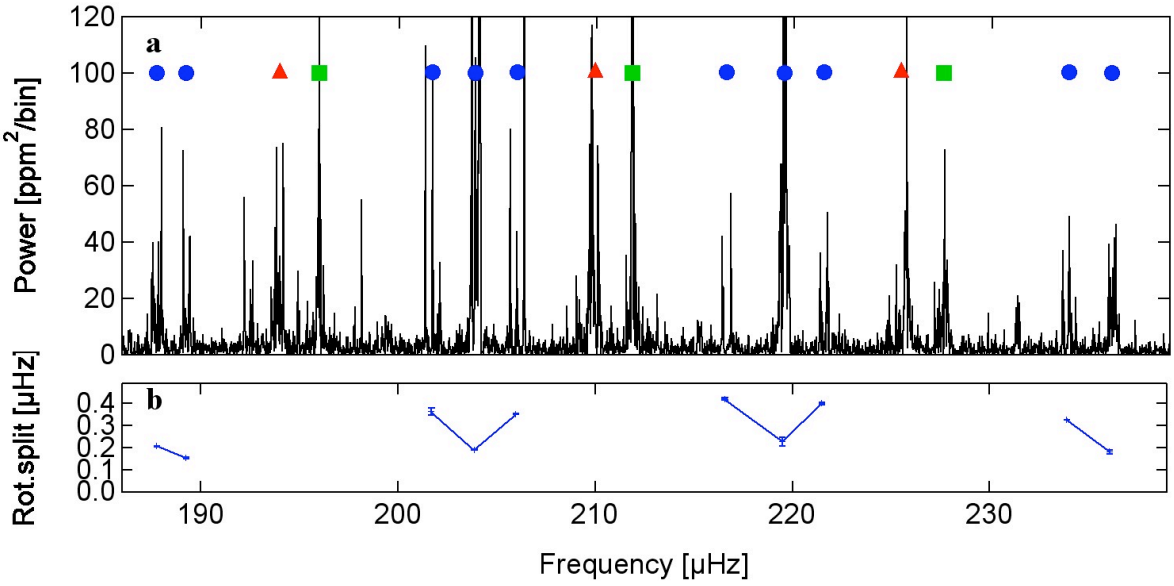

Supplementary Figure 3. Detection of rotational splitting in KIC 5356201. a, Oscillation spectrum and **b,** derived rotational splittings for dipole modes in KIC 5356201. Modes of degree ℓ=0, ℓ=1 and ℓ=2 are represented by green squares, blue dots and red triangles, respectively. The error bars indicate the standard deviation of the measured rotational splitting of dipole modes.

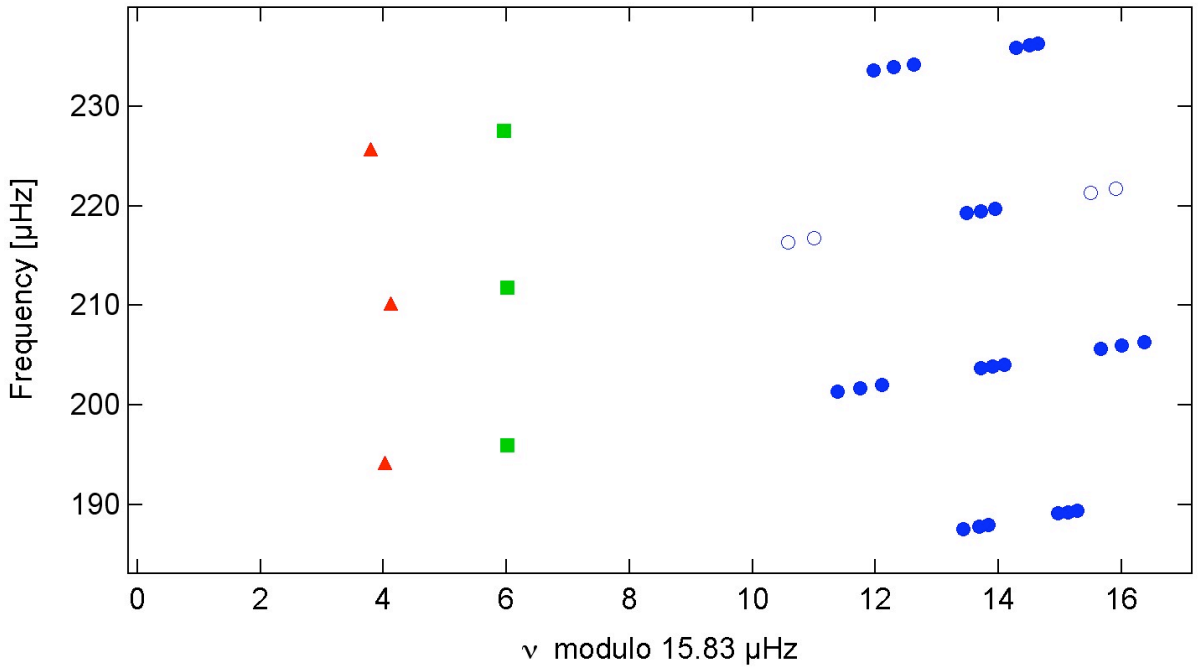

Supplementary Figure 4. The échelle diagram of KIC 5356201. Modes of degree ℓ=0, ℓ=1 and ℓ=2 are marked by green squares, blue dots and red triangles, respectively. Multiplets for which only two peaks with sufficient signal-to-noise were detected in the frequency spectrum are marked with open symbols.

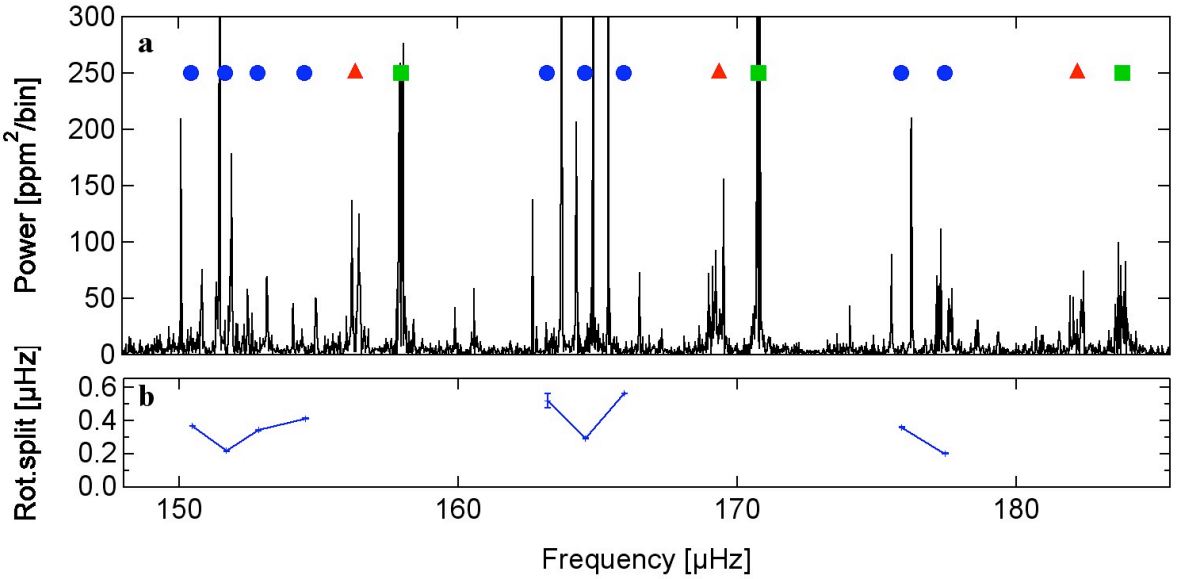

Supplementary Figure 5. Detection of rotational splitting in KIC 12008916. a, Oscillation spectrum and **b,** derived rotational splittings for dipole modes in KIC 12008916. Modes of degree ℓ=0, ℓ=1 and ℓ=2 are represented by green squares, blue dots and red triangles, respectively. The error bars indicate the standard deviation of the measured rotational splitting of dipole modes.

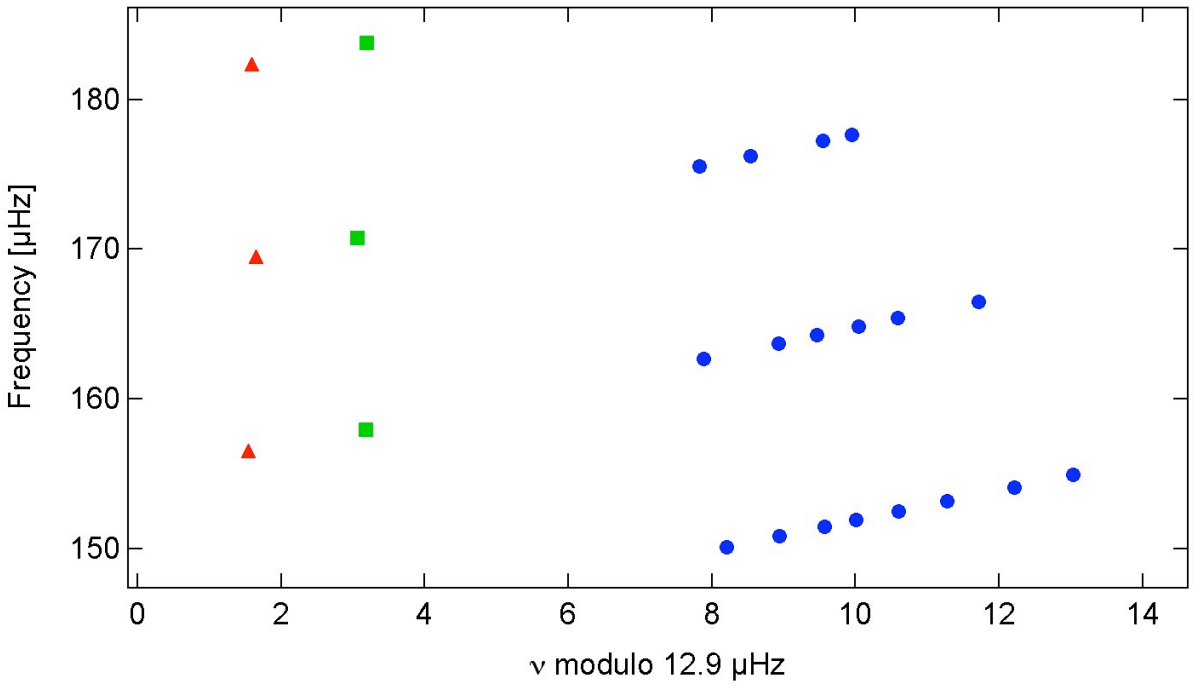

Supplementary Figure 6. The échelle diagram of KIC 12008916. Modes of degree ℓ=0, ℓ=1 and ℓ=2 are marked by green squares, blue dots and red triangles, respectively.

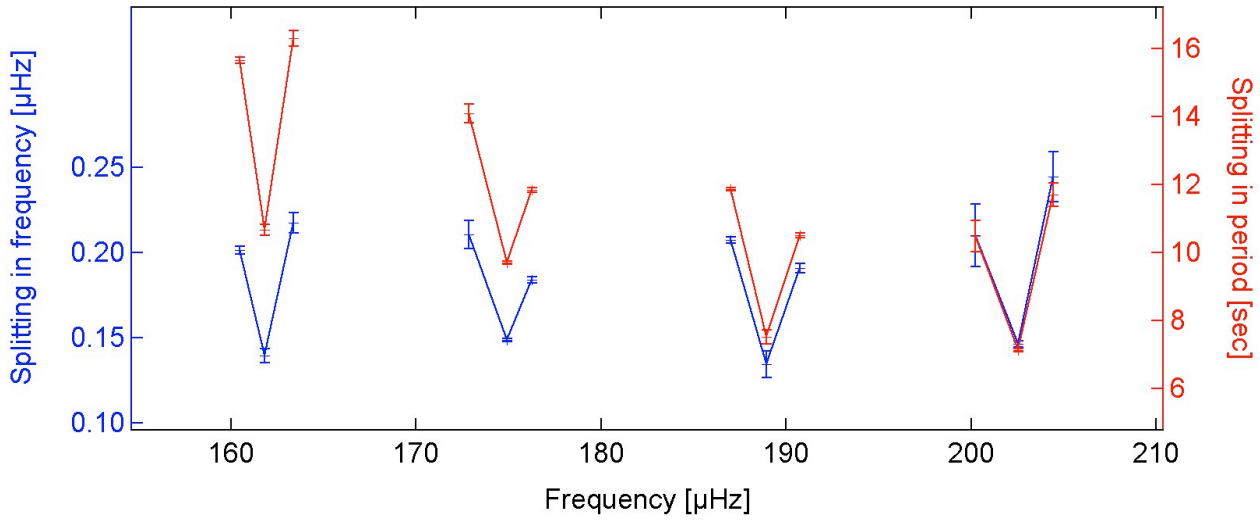

Supplementary Figure 7. Comparison of the separation of split multiplets of dipole modes in KIC 8366239 in the frequency (left-y-axis, blue) and the period domain (right-y-axis, red). For red giants in the H-shell burning phase, the period spacing of rotationally unaffected mixed modes are found to be on the order of about 55 seconds (Ref: 4) which is too large to explain the 5-20 seconds found for rotationally split modes. The error bars indicate the standard deviation of the measured rotational splitting of dipole modes.

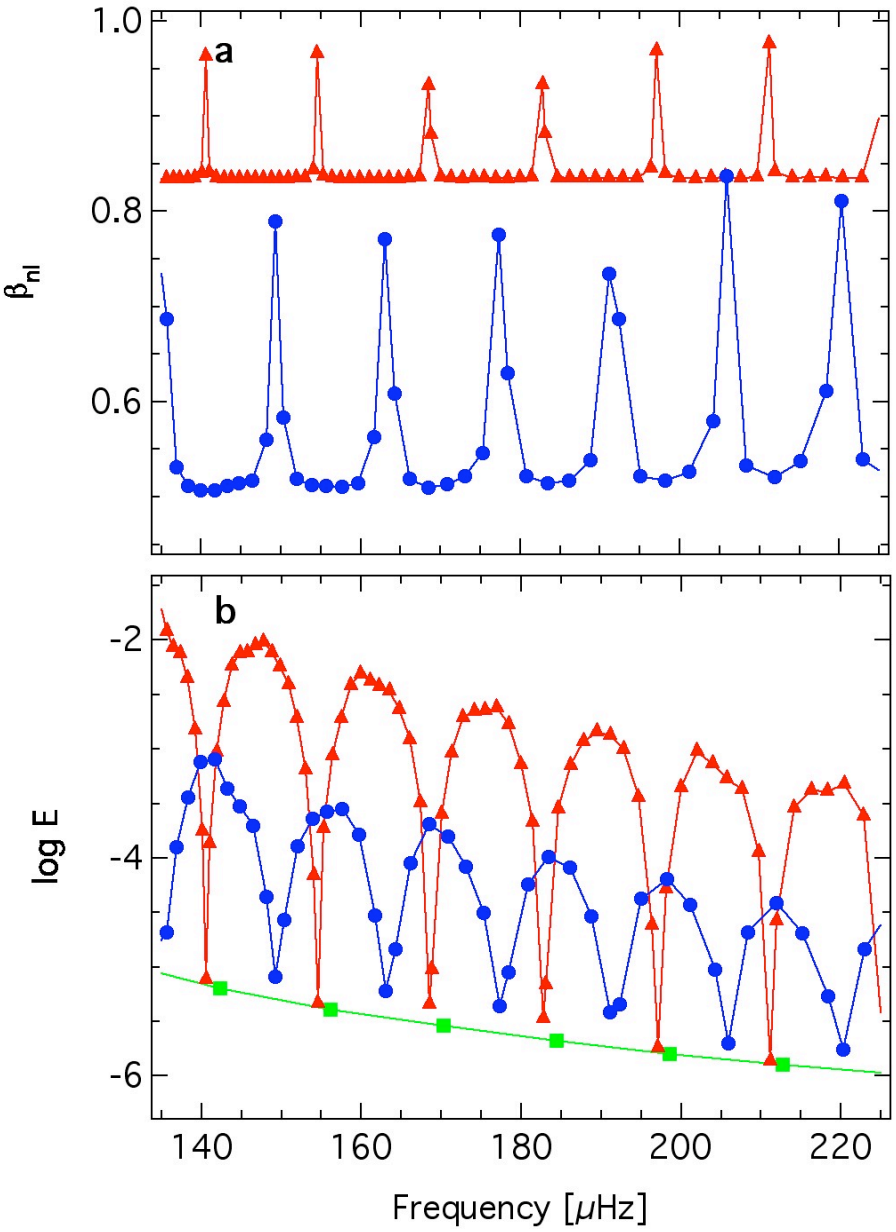

Supplementary Figure 8. The value β_{nl} and mode inertia for a representative stellar model of KIC 8366239. a, β_{nl} as a function of mode frequency for oscillation modes of spherical degree ℓ=1 and ℓ=2 **b,** The corresponding mode inertia log(E) of these modes. Modes of degree ℓ=0, ℓ=1, ℓ=2 are drawn in green, blue, and red, respectively.

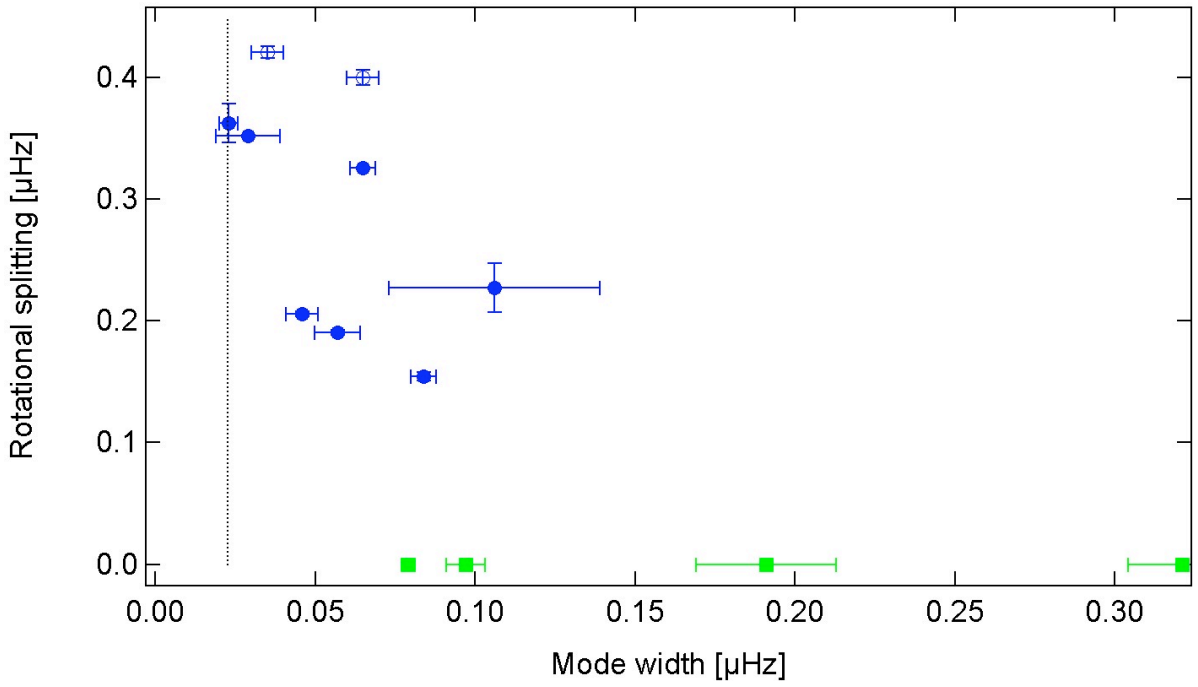

Supplementary Figure 9. Rotational splitting versus mode linewidth for KIC 5356201. Modes of degree ℓ=1 are marked with blue dots. The open blue symbols mark the two modes which only show a doublet structure. For comparison also the linewidths of the pure acoustic radial modes (ℓ=0) are shown with green symbols. The dotted vertical line represents the formal frequency resolution. The error bars indicate the standard deviation of the measured rotational splitting and modewidth of dipole modes.

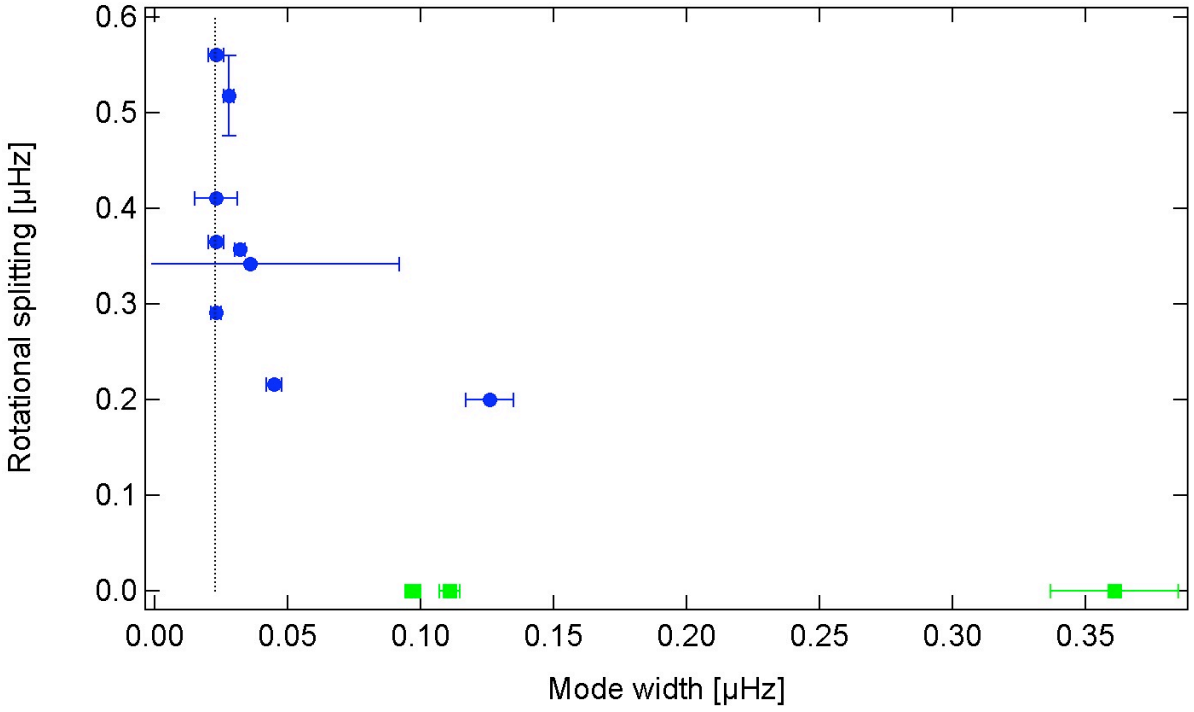

Supplementary Figure 10. Rotational splitting versus modeline width for KIC 12008916. Mode of degree ℓ=1 are marked with blue dots. For comparison also the linewidths of the pure acoustic radial modes (ℓ=0) are shown with green symbols. The dotted vertical line represents the formal frequency resolution. The error bars indicate the standard deviation of the measured rotational splitting and modewidth of dipole modes.

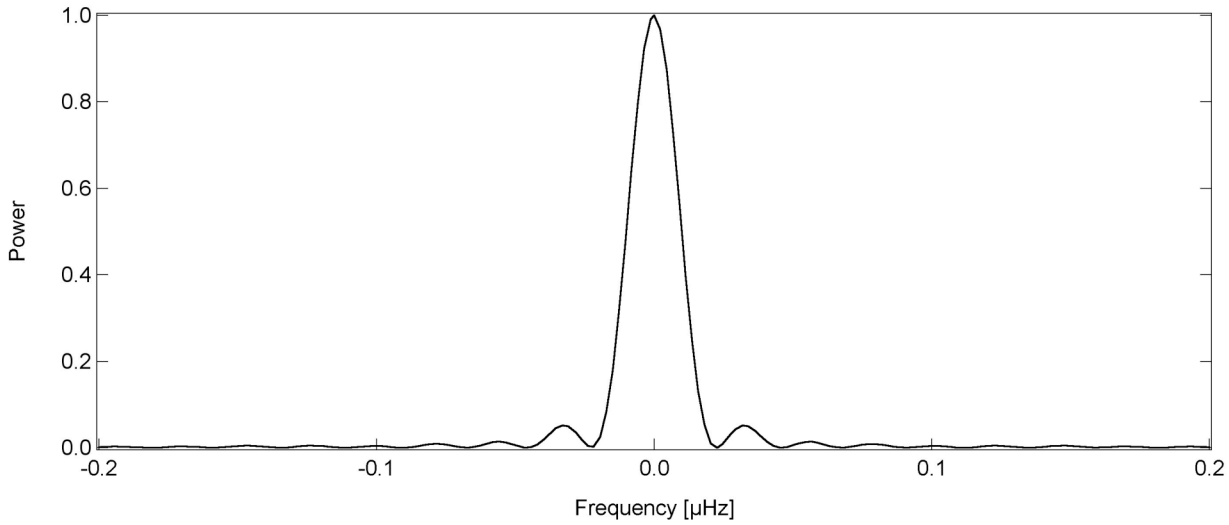

Supplementary Figure 11. The spectral windows of the time series for KIC 8366239. It is identical with the spectral window of the stars KIC 5356201 and KIC 12008916. The nearly uninterrupted dataset of 510 days (quarters Q0-Q6) for each of the stars leads to a spectral window very close to the theoretical single peak distribution.